

# EVAPOTRANSPIRATION MODELING IN FOREST ECOSYSTEM BASED ON SATELLITE THERMAL DATA

Rimjhim Bhatnagar Singh and Ajai  
Forestry, Land-use and Photogrammetry Group  
Remote Sensing and Image Processing Area,  
Space Applications Center, ISRO, Ahmedabad-380015  
**Email:** [rimjhim@sac.isro.gov.in](mailto:rimjhim@sac.isro.gov.in); [ajai@sac.isro.gov.in](mailto:ajai@sac.isro.gov.in)

**KEY WORDS:** Evapotranspiration, LST, Surface emissivity, albedo, net radiation, sensible heat flux

## ABSTRACT:

Energy and mass transport between and within soils, canopies, and the atmosphere is an area of increasing interest in hydrology and meteorology. Evapotranspiration (ET) can account for over 90% of the precipitation, making accurate knowledge of the surface energy balance particularly critical. This paper deals with the evapotranspiration modeling in the forest ecosystem and gives evapotranspiration maps as output. Since, the Energy exchange through the process of evapotranspiration is highly dynamic and depends on a large number of factors, it has been substantially highlighted in this paper. Here, three process-based ET estimation models based on the canopy temperature, derived from satellite thermal channels and the weather parameters, have been described and compared for forest ecosystem. LST and emissivity required for the models are estimated by another sub-model called Temperature-Emissivity separation algorithm using thermal channels of ASTER. The VNIR and SWIR bands of ASTER are used for the estimation of albedo. Net radiation has been estimated using the inputs such as LST, emissivity, albedo, sunshine duration and ambient temperature. Finally, a package has been developed using 'C' language for executing the models proposed.

## 1.0 INTRODUCTION

Energy and mass transport between and within soils, canopies, and the atmosphere is an area of increasing interest in hydrology and meteorology. Recent advances in measurement and modeling have made it possible to accurately estimate evapotranspiration (ET) and the entire surface energy balance. On a global scale, about 64% of the precipitation on the continents is evapotranspired. Of this, about 97% is evapotranspired from land surface and 3% is open-water evaporation (Varni et al. 1999). On arid and semiarid rangelands, ET can account for over 90% of the precipitation, hence, knowledge of the surface energy balance is particularly critical (Flerchinger et al. 1996). This is to say that the greatest amount of water from the hydrologic system is evapotranspired. Evapotranspiration and CO<sub>2</sub> uptake by vegetation are intrinsically coupled leading to links and feedbacks between land surface and climate that have only begun to be explored. (Hutjes et al 1998). Forests strongly influence the global hydrologic and carbon cycles and thus climate (Musselman and Fox, 1991). ET from forest ecosystem is thus essential. In a region, ET varies spatially as well as temporally due to variation in the land cover/vegetation type and conditions and also due to changing weather conditions. Therefore the methods for estimating ET, which are location based, are not appropriate for estimating ET in forest ecosystem and its variability with time. The models based on satellite remote sensing are ideally suited for ET estimation in forests. In this paper, three models for ET estimation are discussed, and compared.

Land-surface temperature (LST), which is an integral input for ET estimation, combines the results of all surface-atmosphere interactions and energy fluxes between the ground and the atmosphere and is therefore a good indicator of the energy balance at the earth's surface. Here, it is calculated using Temperature-emissivity separation algorithm using thermal channels. Albedo is highly variable for different surfaces and for the angle of incidence or slope of the ground surface. Its

estimation is indispensable for radiation budget. Hence, remote sensing data are used to evaluate the surface albedo; land surface temperature and these parameters are then used to estimate evapotranspiration rates.

## 2.0 MODELS USED

ET estimation is quite a complicated and tedious task and hence number of methods using indirect methods lead to its estimation. This has resulted into the development of the models based on energy interactions with the environment. Here, three process-based models are used.

### 2.1 Energy-Balance approach

The heating and evaporation of water requires energy; therefore, the ET process is limited by the input of energy into the system. ET is the one component that links the surface energy balance to the surface water balance, and by knowing the values of the remaining components in either system, it can be computed (Allen et al. 1998). The land surface energy balance leading to evapotranspiration can be described as:

$$R_n - G - LET - H = 0 \quad (1)$$

Where  $R_n$  is net radiation,  $G$  is soil heat flux,  $LET$  is the latent heat flux and  $H$  is the sensible heat flux. All terms are in units of  $J s^{-1}$  and may be positive or negative. The magnitude and sign of the energy balance terms depend on several factors, such as day of the year, time of day, and the condition of the atmosphere (Allen et al. 1998).  $R_n$ ,  $G$ , and  $H$  can all be estimated, thus permitting the computation of the latent heat fluxes as a residual (ET). In equation one, only the vertical

energy fluxes are considered while horizontal fluxes are ignored. As a result, this equation is valid only in homogeneous vegetation cover.

The latent heat flux obtained in this manner is converted to ET using the following expression:

$$AET = LET/L \quad (2)$$

Where, L is latent heat of vaporization of water.

### 2.2 Priestly-Taylor method

One formulation of potential ET that lends itself to remote sensing inputs is that developed by Priestly and Taylor (1972). They modified the Penman equation of ET estimation by approximating the term for aerodynamic resistance and instead introduced coefficient called Priestly-Taylor coefficient. The equation is represented as:

$$LET = a \cdot \frac{Q}{\gamma + \gamma_s} \quad (3)$$

Where,  $\gamma_s$  = slope of derivative of saturated vapor pressure curve, Q = available energy for evapotranspiration,  $\gamma$  = psychrometric constant

The energy available for evapotranspiration is obtained from the energy balance for the land system comprising of the net solar radiation and the ground heat flux.

### 2.3 Bowen ratio method

Bowen ratio is the ratio of sensible heat flux to latent heat flux. It is yet another method for evapotranspiration estimation. Using this method, Latent heat flux is calculated as follows:

$$LET = (R_n - G)/(1 + \beta) \quad (4)$$

$\beta$  is Bowen ratio, a function of saturated vapor pressure. It is represented as

$$\beta = \gamma(T_s - T_a)/(e_s - e_a) \quad (5)$$

While, the Bowen ratio and energy balance approach estimate AET, Priestley-Taylor method gives PET.

## 3.0 INFLUENCES ON EVAPOTRANSPIRATION AND SOURCE OF OBTAINING THEM

### 3.1 Air temperature

The solar radiation absorbed by the atmosphere and the heat emitted by the earth increases the air temperature. The sensible heat of the surrounding air transfers energy to the canopy and exerts as such a controlling influence on the rate of evapotranspiration. Here, air temperature;  $T_a$  is extracted from daily weather report.

### 3.2 Wind speed

The process of vapor removal depends to a large extent on wind and air turbulence, which transfers large quantities of air over the evaporating surface. When vaporizing water, the air above the evaporating surface becomes gradually saturated with water vapor. If this air is not continuously replaced with drier air, the driving force for water vapor removal and the evapotranspiration rate decreases.

For the calculation of evapotranspiration, wind speed measured at 2 m above the surface is required. In this regard, a logarithmic wind speed profile is used for wind speed measurements. It is obtained from the monthly weather report over the study area.

### 3.3 Atmospheric pressure

It is the pressure exerted by the weight of the earth's atmosphere. Evaporation at high altitudes is promoted due to low atmospheric pressure. The effect of Atmospheric pressure is included through the use of psychrometric constant expressed as:

$$\gamma = c_p P / \epsilon \lambda = 0.665 * 10^{-3} P \quad (6)$$

The effect is, however, small and in the calculation procedures, the average value for a location is sufficient

### 3.4 Vapor pressure

The number of water molecules that can be stored in the air depends on its temperature. The higher the air temperature, the higher the storage capacity, the higher its saturation vapor pressure. The slope of the curve changes exponentially with temperature. The derivative of this slope is used for the computation of ET.

$$\Delta = 4098 * e_s / (T + 237.3)^2 \quad (7)$$

### 3.5 Mean saturation vapor pressure

As saturation vapor pressure is related to air temperature, it can be calculated from the air temperature. The relationship is expressed by:

$$e^o(T) = 0.6108 \exp((17.27T)/(T + 237.3)) \quad (8)$$

### 3.6 Net radiation

Energy of the sun incident on the earth on penetrating the atmosphere, is scattered, reflected or absorbed by the atmospheric gases, clouds and dust. The amount of radiation reaching a horizontal plane is known as the solar or short wave radiation,  $R_s$ . The earth then emits radiative energy with wavelengths longer than those from the sun. Therefore, the terrestrial radiation is referred to as long wave radiation. The emitted long wave radiation ( $R_{l, up}$ ) is absorbed by the atmosphere or is lost into space. The long wave radiation received by the atmosphere ( $R_{l, down}$ ) increases its temperature and, as a consequence, the atmosphere radiates energy of its

own. Part of the radiation finds its way back to the earth's surface. Consequently, the earth's surface both emits and receives long wave radiation. The difference between outgoing and incoming long wave radiation is called the net long wave radiation,  $R_n$  and leads to evapotranspiration.

$$R_n = (1-a) R_{sol} + s e_a T_a^4 - e_s T^4 \quad (9)$$

Where,  $s$  = Stefan's constant,  $e_a$  = surface and air emissivity respectively,  $T$ ,  $T_a$  = LST and temperature of the air respectively,  $a$  = albedo,  $R_{sol}$  = solar insolation

### 3.7 Albedo

A considerable amount of solar radiation reaching the earth's surface is reflected. The fraction,  $a$ , of the solar radiation reflected by the surface is known as the albedo. It is highly variable for different surfaces and for the angle of incidence or slope of the ground surface. It is estimated as the average of the spectral reflectance of SWIR and VNIR regions.

### 3.8 Extraterrestrial (solar) radiation

The solar radiation received at the top of the earth's atmosphere on a horizontal surface is called the extraterrestrial (solar) radiation,  $R_a$ . As seasons change, the position of the sun, the length of the day and, hence,  $R_a$  change as well. Extraterrestrial radiation is thus a function of latitude, date and time of day and hence is expressed as:

$$R_a = (24 \cdot 60 / p) R_o \cdot dr [w_s \cdot \sin \delta \cdot \cos \phi + \cos \delta \cdot \sin \phi \cdot \sin w_s] \quad (10)$$

Where,  $R_o$  = solar constant,  $dr$  is inverse relative earth-sun distance and is a function of julian day.

### 3.9 Ground heat flux (G)

In making estimates of evapotranspiration, all terms of the energy balance should be considered. The soil heat flux,  $G$ , is the energy that is utilized in heating the soil. It is driven by a thermal gradient in the uppermost top soil (Parodi, 2000). However, its value is so small compared to other terms so that it is usually ignored.

### 3.10 Sensible heat flux (H)

Sensible heat flux is the heat transferred between the surface and air due to the difference in temperature between them. It is a two-step process as the heat transfer takes place through conduction as well as convection. It is estimated in the following manner:

$$H = \rho C_p (T_s - T_a) / R_a \quad (11)$$

$T_s$  = land surface temperature,  $R_a$  = aerodynamic resistance  
Since, wind plays a significant role in the ET process, hence, it brings in the term,  $R_a$ , aerodynamic resistance which is a function of wind speed.

$$R_a = \ln((z_a - d) / z_{om})^2 / k^2 u_a (1 + 5g(z_a - d)(T_s - T_a) / u_a^2 T_a)^\eta \quad (12)$$

Here,  $z_a$  = height at which air temperature is measured,  $d$  = displacement height =  $0.66z_v$ ,  $z_v$  being the vegetation height,  $z_{om}$  or  $z_o$  = momentum roughness length =  $0.13 z_v$ ,  $k$  = von karman's coefficient =  $0.4$ ,  $u_a$  = wind speed,  $g$  = acceleration due to gravity,  $\eta$  = Stability constant

### 3.11 LST and surface emissivity

Land surface temperatures ( $T$ ) are important in global-change studies, in estimating radiation budgets and heat-balance studies, and as control for climate models. Here, for ET estimation.

Emissivities ( $e$ ) are strongly indicative of composition of the land surface. Surface emissivities are thus important for studies of soil development and erosion and for estimating amounts and changes in sparse vegetative cover for which the substrate is visible. Surface temperatures are independent of wavelength and can be recovered from a small number of bands. Because emissivity spectra can be quite complex, emissivity studies require as many spectral bands in the 8-14 mm TIR window as possible.

Standard Temperature-emissivity separation algorithm, TES, developed by Gillespie et al, 1999 using multiple thermal channels has been used for LST and surface emissivity estimation. The method uses Planck's radiation law in conjunction with Normalized emissivity and maximum-minimum difference approach.

## 4.0 STUDY AREA

The study area is the micro level watershed Moolbury situated in Shimla district of Himachal Pradesh. Figure 1 displays the study area obtained from LISS-4 data.

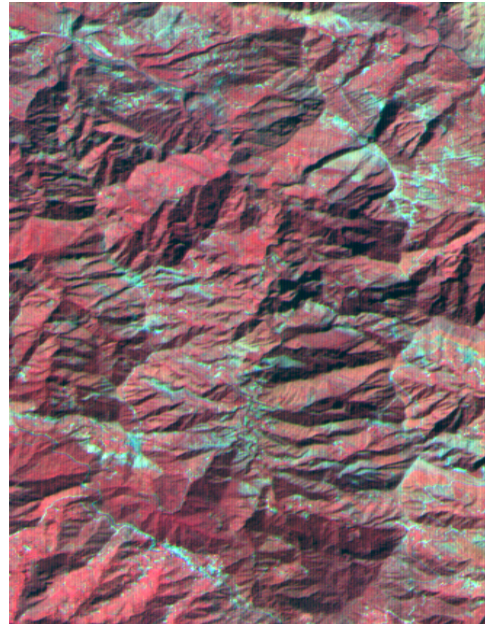


Figure 1: Watershed Moolbari

The watershed lies in outer Himalayas, specifically located in the Satluj river valley. The upper side of it is the cold desert while to the northwest of it is the famous Bhakra-Nangal dam on the river Satluj. The terrain height is around 1300 to 1800m

and is highly undulating. The land cover apart from habitation consists of agricultural land, dense as well as thin forest, scrubland and pastureland. The dominant tree species are Oak and Pine.

### 5.0 DATA USED

Data from ASTER onboard EOS-Terra is used for the present work. ASTER is a multi-spectral scanner that produces images of high spatial resolution. The instrument has three bands in the visible and near-infrared (VNIR) spectral range (0.5-0.9  $\mu\text{m}$ ) with 15-m spatial resolution, six bands in the short-wave infrared (SWIR) spectral range (1.6-2.4  $\mu\text{m}$ ) with 30-m spatial resolution, and five bands in the thermal-infrared (TIR) spectral range (8-12  $\mu\text{m}$ ), with 90-m resolution (Gillespie et al.1999). The VNIR and SWIR channels are used for albedo estimation while TIR channels are used for LST and surface emissivity estimation.

Air temperature, wind speed and Dew point temperature are obtained from Daily weather report supplied by IMD for the said dates.

### 6.0 RESULTS

On executing the TES algorithm, LST and surface emissivity images are obtained. Figures 2, 3 and 4 display the LST images for three consecutive dates 12<sup>th</sup> April 2002, 28<sup>th</sup> September 2002 and 30<sup>th</sup> October 2002 respectively for the study area. As expected, the LST values are higher for barren land and exposed rocks as compared to vegetated areas but, as vegetation is more important in context to ET, so the sample points are taken over the forest site only. Table 1 depicts the change in LST with the change in month over ten sample points selected randomly over the site. Figure 5 show the comparison between ET obtained from different methods for 12<sup>th</sup> April 2002 while figures 6 and 7 respectively display the ET images for 28<sup>th</sup> September 2002 and 30<sup>th</sup> October 2002. Tables 2, 3 and 4 compare the ET values of the ten sample points selected over the watershed. The darker regions in the LST images depict low values of temperature while lighter shades of gray show high temperature. On the contrary, ET images display high values for darker regions and vice-versa.



Figure 2:LST image for 12<sup>th</sup> April 2002



Figure 3:LST image for 28<sup>th</sup> September 2002



Fig 4:LST image for 30<sup>th</sup> October 2002

S. No	LST in K for 12 <sup>th</sup> April 2002	LST in K for 28 <sup>th</sup> Sept. 2002	LST in K for 30 <sup>th</sup> October 2002
1.	295	290	289
2.	295	286	286
3.	298	292	291
4.	295	290	288
5.	297	290	289
6.	301	294	293
7.	295	289	288
8.	298	287	287
9.	297	292	291
10.	299	293	291

Table 1:Comparison between LST for different months



Figure 6:ET image for 12<sup>th</sup> April 2002 using Energy Balance



Fig 7:ET image for 28<sup>th</sup> Sept. 2002 using Energy Balance



Fig 8:ET image for 30<sup>th</sup> October 2002 using Energy Balance

## 6.0 DISCUSSIONS AND CONCLUSIONS

During this work, three remote sensing based models for ET estimation and one model for LST estimation has been tested whose results are tabulated. Land surface temperature, as expected, declined from April to October as the winter approach, for the months considered in the study resulting in the change in net radiation available for ET. But, as, meteorological factors also contribute to ET so the ET pattern cannot be predetermined.

Tables 2, 3 and 4 give a clear-cut comparison of change in ET values with the time of the year.

S.No	ET in mm/day for 12 <sup>th</sup> April 2002	ET in mm/day for 28 <sup>th</sup> Sept. 2002	ET in mm/day for 30 <sup>th</sup> Oct. 2002
1.	5.87	5.14	6.11
2.	5.89	3.05	4.12
3.	6.66	5.77	6.85
4.	5.87	5.16	5.65
5.	6.4	5.16	6.1
6.	7.42	6.34	7.45
7.	5.88	4.78	5.65
8.	6.65	3.81	5.04
9.	6.4	5.77	6.88
10.	6.92	6.05	6.87

Table 2:Comparison between ET for different months for Energy balance approach

S.No	ET in mm/day for 12 <sup>th</sup> April 2002	ET in mm/day for 28 <sup>th</sup> Sept. 2002	ET in mm/day for 30 <sup>th</sup> Oct. 2002
1.	4.2	4.13	6.01
2.	4.21	3.65	5.57
3.	4.58	4.38	6.32
4.	4.2	4.15	5.86
5.	4.45	4.15	6.0
6.	4.97	4.65	6.63
7.	4.2	4.01	5.86
8.	4.57	3.77	5.72
9.	4.45	4.38	6.34
10.	4.7	4.51	6.33

Table 3:Comparison between ET for different months for Bowen ratio method

S.No	ET in mm/day for 12 <sup>th</sup> April 2002	ET in mm/day for 28 <sup>th</sup> Sept. 2002	ET in mm/day for 30 <sup>th</sup> Oct. 2002
1.	5.53	5.37	6.19
2.	5.55	4.73	5.74
3.	6.03	5.69	6.5
4.	5.53	5.38	6.04
5.	5.86	5.38	6.17
6.	6.55	6.03	6.83
7.	5.54	5.21	6.04
8.	6.02	4.89	5.88
9.	5.86	5.69	6.53
10.	6.2	5.86	6.52

Table 4:Comparison between ET for different months for Priestley-Taylor relation

As can be seen the values are apparently different though slightly. This change may be attributed to the variety of factors including climatic. This analysis is important and needs attention. Hence, this is planned in the future work following ground measurement of ET using sap flow meter.

#### **ACKNOWLEDGEMENT**

We are thankful to Mr. Shailendra Singh and Mr. Ritesh Agrawal for their help in the writing of the software whenever required.

#### **REFERENCES**

Allen, R. G., Pereira, L. S., Raes, D., & Smith, M., 1998. Crop evapotranspiration: Guidelines for computing crop water requirements, FAO Irrigation and Drainage Paper, vol. 56. Rome, Food and Agriculture Organisation of the United Nations, 300 pp.

Flerchinger G. N., Hanson C. L., and Wight J. R. Modeling evapotranspiration and surface energy budgets across a watershed Water Resources Research, vol. 32, no. 8, pages 2539–2548, August 1996

Gillespie A.R., Rokugawa S., Hook S.J., Matsunaga T and A. B. Kahle, 1999. Temperature/Emissivity Separation Algorithm Theoretical Basis Document, Version 2.4

Hutjes, R.W.A. et al, 1998 Biospheric aspects of the hydrological cycle. J.of Hydrology,(212-213):1-21.

Musselman, R.C. , Fox, D.G., 1991. A review of the role of temperate forests in the global CO<sub>2</sub> balance. Journal of air waste management association 41, 798-807

Parodi, G., 2000.AVHRR Hydrological Analysis system- Algorithms and theory-Version-1.0.WRES, ITC, The Netherlands.

Varni, M., Usunoff, E., Weinzettel, P., & Rivas, R. 1999. The groundwater recharge in the Azul aquifer, central Buenos Aires Province, Argentina, Physics and Chemistry of the Earth, 24(4), 349– 352.